Hydrogen Bonding-Directed Metallosupramolecular Structural Motifs Based on a Peripheral Urea Fused Bipyridine Tecton

ARTICLE *in* CRYSTAL GROWTH & DESIGN · MAY 2008

Impact Factor: 4.89 · DOI: 10.1021/cg8000015

3 AUTHORS, INCLUDING:

Megha Subhash Deshpande
Nara Institute of Science and Technology
14 PUBLICATIONS **217** CITATIONS
SEE PROFILE

Vedavati G Puranik
CSIR - National Chemical Laboratory, Pune
225 PUBLICATIONS **2,864** CITATIONS
SEE PROFILE

CRYSTAL GROWTH & DESIGN
2008
VOL. 8, NO. 6
1952–1960

Hydrogen Bonding-Directed Metallosupramolecular Structural Motifs Based on a Peripheral Urea Fused Bipyridine Tecton

Megha S. Deshpande,[†] Avinash S. Kumbhar,*[,†] and Vedavati G. Puranik[‡]

Department of Chemistry, University of Pune, Pune - 411 007, India, and Center for Materials Characterization, National Chemical Laboratory, Pune - 411 008, India

Received January 1, 2008; Revised Manuscript Received February 14, 2008

ABSTRACT: The potential of bipyridine glycoluril (BPG), a urea fused bipyridine, tecton to form metal−organic frameworks (MOFs) has been explored by structural characterization of BPG and its complexes $[Ru(phen)(BPG)_2]Cl_2$ (**1**) and $[Ru(BPG)_3]Cl_2$ (**2**). The single crystal X-ray structure of BPG reveals that the inherent H-bond donor (N−H) and acceptor groups (C═O) exhibit a potential to generate diverse supramolecular motifs depending on the stoichiometry of tectons. The single crystal X-ray analysis of the secondary building units **1** and **2** provide evidence for this hydrogen-bonding capacity which results in supramolecular self-assembled metal−organic frameworks (MOF) via C−H···Cl, C−H···O, N−H···Cl, and N−H···O interactions with a cluster of water molecules and chlorine anions surrounding secondary building units in **1** and channels encapsulating mixed water−dimethylsulfoxide clusters in **2**.

Introduction

Metallosupramolecular chemistry which involves the interplay between organic and metallic tectons can be used to design network materials with predefined dimensional (1D, 2D, or 3D) structural motifs.[1–3] The major approaches to such materials that have been employed are noncovalent interactions such as hydrogen-bonding, metal-ion coordination, electrostatic and hydrophobic forces.[1–3] Formation of such supramolecular metal−organic frameworks (MOF) structures has attracted much attention in recent years due to their applications in diverse areas such as catalysis, optoelectronics, supramolecular storage of molecules, molecular recognition, and magnetism.[4–8]

A commonly used strategy in building such extended network structures is to employ appropriate bridging ligands, which on complexation with metal ions forms "supramolecular glue" resulting in polymer networks with channels, voids, and porous structures encapsulating solvent molecules.[9] Among widely used bridging ligands are 4,4′-bipyridine, 1,2-bis(4-pyridyl)ethane, 1,2-bis(4-pyridyl)ethene, 1,3-bis(4-pyridyl)-propane, urea fused pyridine derivatives such as *N,N*′-bis(*m*-pyridyl)urea, *N,N*′-bis(*m*-cyanophenyl)urea, and multidentate aromatic polycarboxylates.[9]

However, in most of the cases the MOFs are formed by hydrothermal/solvothermal methods wherein limited control can be achieved by the appropriate selection of organic ligands and metal salts. For example, some combinations of labile metal ions and organic donor atoms viz. Pd(II) or Ag(I) and pyridine nitrogen donors are common in the literature. However, the examples of the incorporation of the less labile metal ion such as ruthenium(II) using this "metal ion as glue approach" are rare.

Another approach to forming such networks is to use a chelating ligand with additional H-bonding groups, coordination sites, or extended π-functionality. The majority of MOF structures of this type rely on 2,2′-bipyridine derivatives with hydrogen bonding groups such as carboxylic acids, alcohols, amides, and amines which form extended H-bonding network structures.[10] This approach allows the use of inert metal ion−ligand combinations as the metal complex as a whole behaves as a supramolecular synthon generating 3D architectures.

Scheme 1. Urea-Fused Bipyridine-Glycoluril Ligand Showing the Hydrogen-Bonding Sites

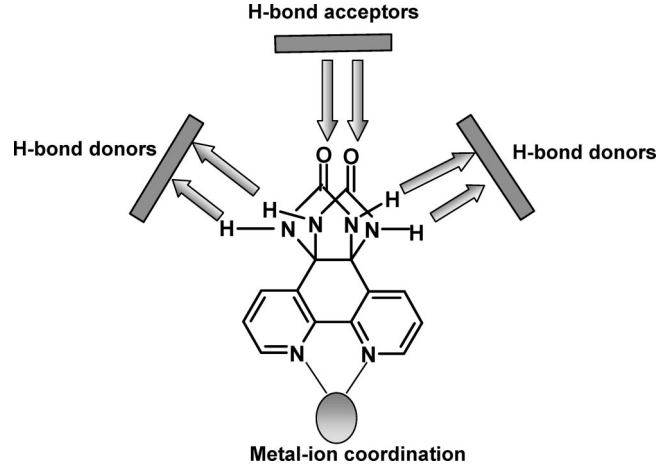

As a part of our research program in the area of MOFs, we have explored this possibility by using the bidentate urea fused bipyridine ligand with the 2,2′-bipyridine chelating group and the peripheral H-bonding urea groups (Scheme 1). Recently, we have reported the supramolecular self-assembled ruthenium(II) polypyridyl framework $[Ru(bpy)_2(BPG)]Cl_2$ (where BPG = bipyridine-glycoluril) which encapsulates discrete water clusters[11a] and have demonstrated that these urea groups are also involved in DNA binding facilitating hydrolytic cleavage by this complex.[11b] Also the BPG ligand has been utilized previously as a tecton which forms an octahedrally coordinated secondary building block with Fe(II) which self-assembles through hydrogen bonding to a nanoporous network.[12] In the present work we report the syntheses and structural characterization of BPG and its complexes $[Ru(phen)(BPG)_2]Cl_2$ (**1**) and $[Ru(BPG)_3]Cl_2$ (**2**) and demonstrate the diverse nature of

* E-mail: askum@chem.unipune.ernet.in; tel: (+91) - 020 - 25601225 (534); fax: (+91) - 020 - 25691728.
[†] University of Pune.
[‡] National Chemical Laboratory.

10.1021/cg8000015 CCC: $40.75
Published on Web 05/06/2008

Scheme 2. Synthetic Route for Tecton BPG and Its Ruthenium(II) Complexes Containing One, Two, and Three Tectons

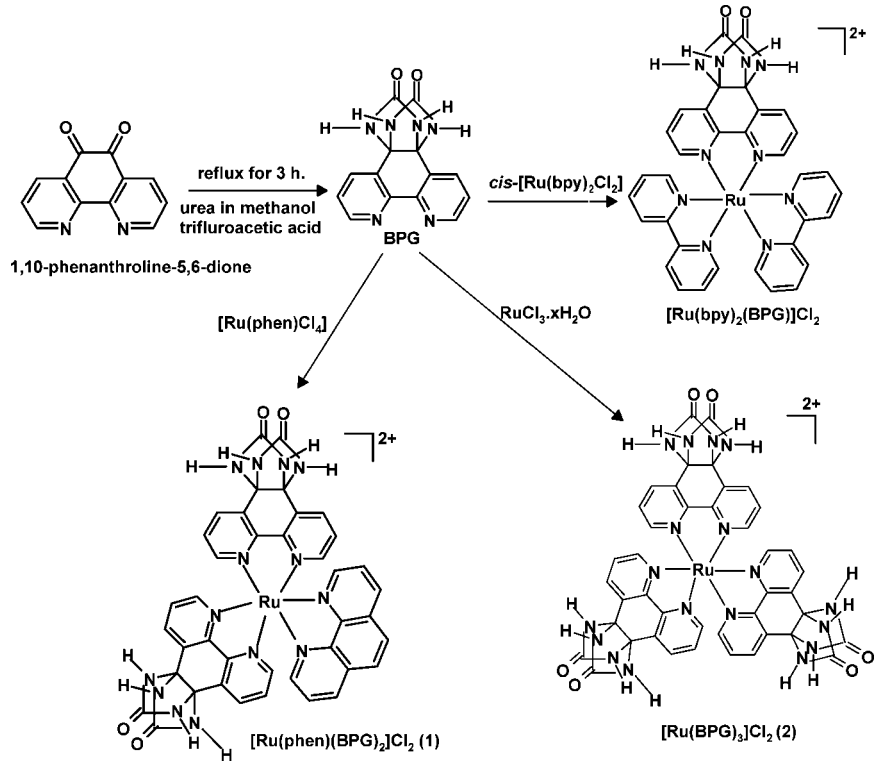

frameworks that can be formed by the variation of the number of the BPG ligands using conventional synthetic methods (Scheme 2).

Experimental Procedures

General. All reagents and solvents were purchased commercially and were used as received. $RuCl_3 \cdot xH_2O$, 1,10-phenanthroline was obtained from S. D. Fine Chemicals Limited (India). The microanalyses (C, H, and N) were carried out with a Perkin-Elmer 240 Q elemental analyzer at NCL, Pune. UV–vis spectra were recorded on a Shimadzu UV-1601 spectrophotometer. Steady-state emission spectra were carried out on a Shimadzu RF-5301 spectrofluorometer at room temperature. ^{1}H NMR spectra were measured on a Varian-Mercury 300 MHz spectrometer with DMSO-d_6 as a solvent at room temperature, and all chemical shifts are given relative to TMS. The infrared spectra of solid samples dispersed in KBr were recorded on a Shimadzu FTIR-8400 spectrophotometer. Thermogravimetric analyses for **1** and **2** were performed on a Mettler Toledo Star System in N_2 atmosphere at a scan rate of 10 °C min^{-1}.

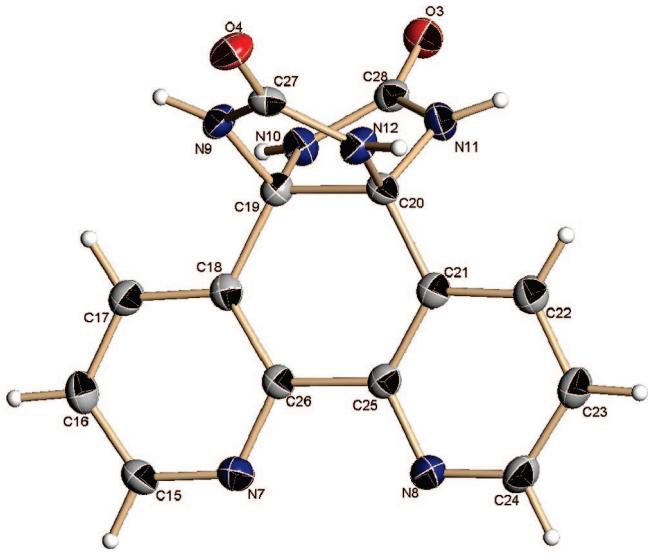

Figure 1. ORTEP diagram of the tecton BPG showing the atom numbering scheme (thermal ellipsoids are drawn at 50% probability).

Syntheses. The ligand 1,10-phenenthroline-5,6-dione (phendione)[13] was synthesized according to the literature protocol. BPG [4b,5,7,7a-tetrahydro-4b,7a-epiminomethanoimino-6H-imidazo[4,5-f] [1,10] phenanthroline-6,13-dione] was prepared by modifying the literature method,[12,14] and the precursor complex $[Ru(phen)Cl_4]$[15] was prepared by using the literature method.

BPG (Tecton). Condensation of 1,10-phenanthroline-5,6-dione (0.5 g, 2.38 mmol) and urea (0.35 g, 5.83 mmol) in methanol with trifluoroacetic acid (2.71 g, 23.78 mmol) yielded 60% of BPG, as an insoluble white powder, washed with water and diethyl ether, and then dried under vaccum. Single crystals of BPG were grown by slow evaporation of the dimethylsulfoxide solution.

Elemental analysis calcd. for $C_{14}H_{10}N_6O_2 \cdot 2H_2O$: C 50.86; H 4.27; N 25.44%; Found: C 51.54; H 4.33; N 25.75%; ^{1}H NMR (DMSO-d_6 solvent, room temperature, ppm) δ = 8.72 (d, 2H), 8.31 (s,4H), 8.06 (d,H), 7.54 (dd,2H); I.R. (KBr cm^{-1}) C═O (1695), N−H (3209), O−H (3418), C═N (1581), C═C (1450); mp > 330 °C.

$[Ru(phen)(BPG)_2]Cl_2 \cdot 4.4\ H_2O$ (1). The precursor complex $[Ru(phen)Cl_4]$ (0.100 g, 0.24 mmol) and BPG (0.139 g, 0.48 mmol) in a 1:2 molar ratio were refluxed in 50% methanol−50% water (50 mL) for 8 h, whereupon the color of the solution changed from dark green to red. The red solution was filtered hot and was cooled to room temperature. After evaporation of the solvent, the brownish red solid was collected and washed with small amounts of methanol and diethyl ether and then dried under vacuum. The product was purified by column chromatography on active alumina using acetone and methanol as eluent. The red fraction was collected and concentrated in vacuum, a small amount of diethyl ether was added to the concentrated solution, and red solid was obtained. Single crystals were grown by slow evaporation of the methanol–water solution.

Yield: (70%); elemental analysis calcd. for $RuC_{40}H_{36.8}N_{14}O_{8.4}Cl_2$ (1019.59): C 47.08, H 3.64, N 19.23%. Found: C 47.63, H 3.83, N 19.63%. ^{1}H NMR (300 MHz, DMSO-d_6, 25 °C, δ): 8.57(m, 6H), 8.33(s, 8H), 8.17(s, 2H), 8.05(d, 2H), 7.97(d, 3H), 7.70(m, 3H), 7.54 (d, 2H), 7.27 (d, 2H). I.R. (KBr, cm^{-1}): C═O (1703), N−H (3207), O−H

Table 1. Crystallographic Data and Structure Refinement for BPG, 1, and 2

compound	BPG	1	2
empirical formula	$C_{28.50}H_{24.50}N_{12}O_6$	$C_{40}H_{42.50}ClN_{14}O_{12.75}Ru$	$C_{48}H_{53}Cl_2N_{18}O_{13}RuS_3$
formula weight	631.10	1059.90	1358.23
T (K)	293(2)	293(2)	293(2)
wavelength (Å)	0.71073	0.71073	0.71073
crystal system	monoclinic	tetragonal	monoclinic
space group	$P2_1/c$	$P42/n$	$C2/c$
a (Å)	18.5018(1)	16.477(5)	23.3557(17)
b (Å)	12.3851(7)	16.477(5)	12.2784(9)
c (Å)	12.6579(7)	20.313(8)	21.6974(16)
β (deg)	108.788(1)		108.5950(10)
V (Å^3)	2746.0(2)	5515(3)	5897.4(7)
Z	4	4	4
d_{calc} (mg/m^{-3})	1.527	1.276	1.530
μ (MoKα) (mm^{-1})	0.113	0.398	0.539
F(000)	1310	2174	2788
crystal size (mm)	0.25 × 0.18 × 0.04	0.36 × 0.17 × 0.11	0.34 × 0.28 × 0.22
θ range (°)	2.01 to 24.99	2.01 to 25.00	2.23 to 25.00
reflections collected/unique	20365/4822 [R(int)= 0.0534]	29784/4687 [R(int) = 0.0953]	14718/5191 [R(int) = 0.0197]
completeness to θ = 25%	99.9	96.4	99.9
max and min transmission	0.9951 and 0.9720	0.9582 and 0.8715	0.8906 and 0.8379
refinement method	full-matrix least-squares on F^2	full-matrix least-squares on F^2	full-matrix least-squares on F^2
GOF on F^2	1.053	0.960	1.103
R1, wR2 [$I > 2\sigma(I)$]	0.0514, 0.1336	0.0656, 0.1862	0.0635, 0.1912
R1, wR2 (all data)	0.0662, 0.1430	0.1194, 0.2072	0.0686, 0.1971

Table 2. Selected Bond lengths (Å) and Angles (°) for BPG

O(1)−C(13)	1.222(3)	O(3)−C(28)	1.228(3)
O(2)−C(14)	1.225(3)	O(4)−C(27)	1.237(3)
N(1)−C(1)	1.334(3)	N(7)−C(15)	1.328(3)
N(1)−C(12)	1.340(3)	N(7)−C(26)	1.349(3)
N(2)−C(10)	1.330(3)	N(8)−C(24)	1.328(3)
N(2)−C(11)	1.354(3)	N(8)−C(25)	1.342(3)
N(3)−C(13)	1.366(3)	N(9)−C(27)	1.350(3)
N(3)−C(6)	1.435(3)	N(9)−C(19)	1.455(3)
N(4)−C(13)	1.355(3)	N(10)−C(28)	1.375(3)
N(4)−C(5)	1.450(3)	N(10)−C(19)	1.448(3)
N(5)−C(14)	1.370(3)	N(11)−C(28)	1.340(3)
N(5)−C(5)	1.442(3)	N(11)−C(20)	1.446(3)
N(6)−C(14)	1.346(3)	N(12)−C(27)	1.343(3)
N(6)−C(6)	1.455(3)	N(12)−C(20)	1.440(3)
O(1)−C(13)−N(4)	125.7(2)	N(12)−C(27)−N(9)	109.1(2)
O(1)−C(13)−N(3)	126.3(2)	O(4)−C(27)−N(9)	125.4(2)
O(2)−C(14)−N(6)	127.1(2)	O(4)−C(27)−N(12)	125.5(2)
O(2)−C(14)−N(5)	124.6(2)	O(3)−C(28)−N(11)	126.2(2)
O(2)−C(14)−N(6)	127.1(2)	O(3)−C(28)−N(10)	125.1(2)

(3408), C═N (1616), C═C (1452). UV–visible (H_2O), λ_{max} nm (log ε): 457 (4.11), 375.5 (3.87), 301 (4.43), 262.5 (4.72), 224 (4.70), 205 (4.84). λ_{em} = 609 nm.

[Ru(BPG)$_3$]Cl$_2$·4H$_2$O (2). This complex was prepared by the reaction of $RuCl_3 \cdot xH_2O$ (0.100 g, 0.44 mmol) and BPG (0.392 g, 1.33 mmol) in a 1:3 molar ratio in 1:1 methanol/water at reflux for 12 h whereupon the color of the solution changed to red. The resulting red solution was cooled to room temperature and filtered. After evaporation of the solvent, the complex was collected, and washed with water and diethyl ether. The product was purified by column chromatography on active alumina using methanol and water as eluent. The red fraction was collected. Single crystals were grown by slow evaporation of the dimethylsulfoxide−water solution.

Yield: (75%); elemental analysis calcd. for $RuC_{42}H_{38}N_{18}O_{10}Cl_2$-(1126.43): C 44.71, H 3.39, N 22.36%; found: C 44.35, H 3.09, N 22.63%; ^{1}H NMR (300 MHz, DMSO-d_6, 25 °C): δ = 8.79 (s, 6H), 8.50 (s, 6H), 8.28 (d, 6H), 7.79 (d, 6H), 7.75 (d, 6H) ppm; ^{1}H NMR (300 MHz, D_2O, 25 °C): δ = 8.15 (d, 6H), 7.90(d, 6H), 7.57(d, 6H) ppm; IR (KBr, cm^{-1}) C═O (1703), N−H (3213), O−H (3417), C═N (1643), C═C (1454). UV–visible (H_2O), λ_{max} nm (log ε): 456 (4.10), 304 (4.48), 262 (4.29), 231 (4.52). λ_{em} = 596 nm.

X-ray Data Collection and Structure Determinations. Data for the compounds BPG, **1** and **2** were collected on a Bruker SMART APEX CCD diffractometer using Mo Kα radiation at room temperature. SHELX-97 (ShelxTL)[16] was used for structure solution and full matrix least-squares refinement on F^2. All the data were corrected for Lorentzian, polarization, and absorption effects. For BPG colorless plate of approximate size 0.25 × 0.18 × 0.04 mm was used for data collection. Crystal to detector distances 6.05 cm, 512 × 512 pixels/frame, multiscan data acquisition. Total scans = 4, total frames = 1968, oscillation/frame –0.3°, exposure/frame = 20.0 s/frame, maximum detector swing angle = −30.0°, beam center = (260.2, 252.5), in plane spot width = 1.24, SAINT integration, θ range = 2.01 to 24.99°, completeness to θ of 24.99° is 99.9%. Hydrogen atoms were included in the refinement as per the riding model. X-ray analysis revealed that there are two molecules in the asymmetric unit along with two water molecules as solvent of crystallization. For **1** brownish red colored rectangular crystal of approximate size 0.36 × 0.17 × 0.11 mm was selected for data collection. All the atoms were refined anisotropically. Hydrogen atoms for the cations were included in the refinement as per the riding model. Hydrogen atoms for some of the water molecules were obtained by a difference map and were refined keeping the isotropic thermal parameters fixed. The asymmetric unit of **1** contains half-molecules of the cations (other half-being generated by symmetry) and one chlorine atom with half-occupancy as anion and nine solvent–water molecules with different occupancies of crystallization in the asymmetric unit. Water molecule O3 is disordered. For **2** red-colored rectangular crystal of approximate size 0.34 × 0.28 × 0.22 mm was grown by slow evaporation of compound in dimethylsulfoxide solution at room temperature and was selected for data collection. The asymmetric unit of **2** contains one molecule of the cation and two chlorine anions along with one and half-dimethylsulfoxide molecules and four water molecules (with half-occupancy) as solvent of crystallization. Out of this, one solvent dimethylsulfoxide molecule having half-occupancy is disordered. All the atoms were refined anisotropically except the C and O atoms of disordered dimethylsulfoxide. Hydrogen atoms for the water molecules were confirmed by a difference map.

Results and Discussion

Syntheses and Properties. The BPG ligand (Scheme 1) was prepared by acid catalyzed condensation of 1,10-phenanthroline-5,6-dione and urea in methanol in good yield. Its composition was characterized by elemental analysis, ^{1}H, ^{13}C NMR spectra and melting point.[11a] The ligand was not soluble in most of the organic solvents but was relatively soluble in dimethylsulfoxide. Secondary building units [Ru(phen)(BPG)$_2$]Cl$_2$ (**1**) and [Ru(BPG)$_3$]Cl$_2$ (**2**) were synthesized as shown in Scheme 2 by reacting BPG with the appropriate precursors followed by chromatographic purification using an alumina column and obtained in a racemic form. The compounds were characterized by using IR, ^{1}H NMR, and elemental analysis. The infrared

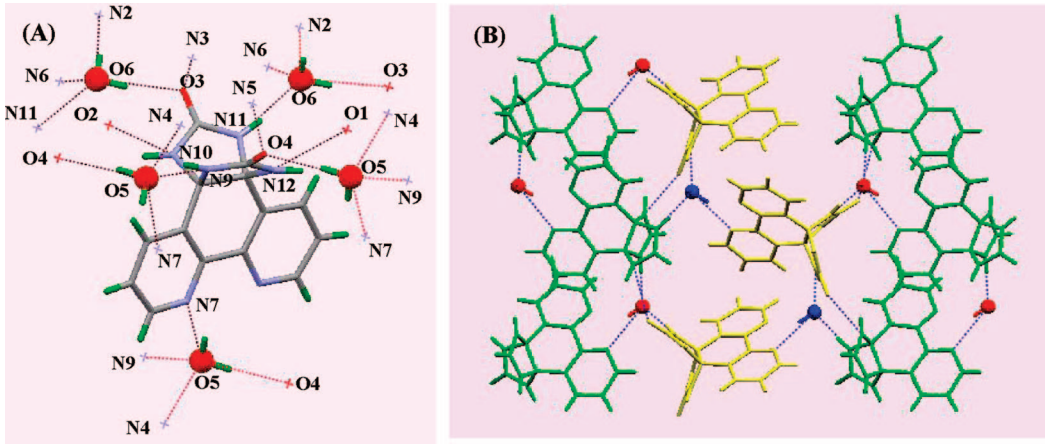

Figure 2. (A) Variegated H-bonding network structure of bipyridine-glycoluril; (B) the organic framework structure of BPG viewed down *a*-axis in the plane showing N−H···O and O−H···N interactions.

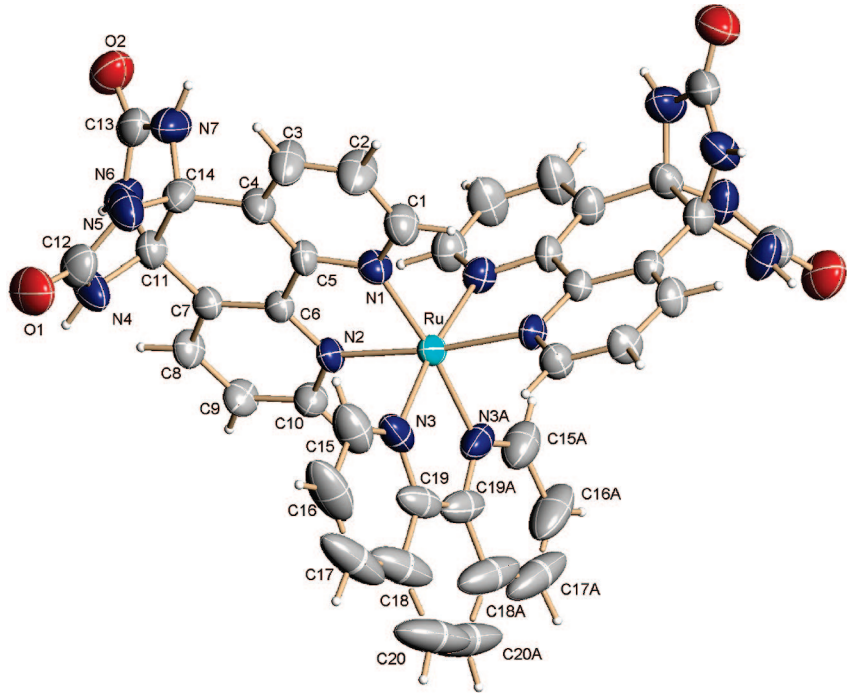

Figure 3. ORTEP diagram of the cationic building block of the composition $[Ru(phen)(BPG)_2]^{2+}$ **1** showing the atom numbering scheme (thermal ellipsoids are drawn at 40% probability).

spectra of tecton BPG and compounds **1** and **2** show a strong band at around 1695–1705 cm^{-1} due to the carbonyl stretching frequency. The tecton BPG show bands at 3209 $cm^{-1}$and 3418 cm^{-1}, and compounds **1** and **2** shows bands at around 3205–3217 cm^{-1} and 3405–3417 cm^{-1} due to the N−H stretching frequencies and O−H stretching frequency of water molecules respectively. The electronic absorption spectra of complexes **1** and **2** are dominated by two sets of transitions (i) low energy metal-to-ligand charge transfer (MLCT) transitions in the range 440–460 nm and (ii) high energy ligand-centered $\pi-\pi^*$ transitions (IL) in the range 200–380 nm for all complexes which are similar to the parent $[Ru(bpy)_3]^{2+}$ and other Ru(II) polypyridyl complexes[17,18a] and emits in aqueous solution at room temperature with maximum 609 and 596 nm respectively. The chelating ability as well as H-bonding capacity of tecton BPG is evidenced by single crystal X-ray structure of BPG and the secondary building units **1** and **2**.

Crystal Structure of BPG. Crystals of BPG suitable for a single-crystal X-ray structure were grown by slow evaporation of the dimethylsulfoxide solution at room temperature. An ORTEP representation of BPG depicted in Figure 1 shows inherent four hydrogen bond donor (N−H) and two acceptor (C═O) groups. Selected data collection parameters, bond lengths and angles are summarized in Tables 1 and 2, respectively. X-ray analysis revealed that there are two molecules in the asymmetric unit extensively hydrogen bonded with each other (N−H···O, C−H···O, N−H···N, C−H···N, O−H···N) and also with two water molecules (Figure 2A, Table S1 and Figure S1 in the Supporting Information). Out of the four N−H groups of one ligand molecule two N−H groups H-bond with carbonyl C═O group of the symmetry related molecule and the remaining two N−H groups H-bond with two water molecules. A similar nature is repeated by the other molecule in the asymmetric unit. Also it shows an additional H-bond between the chelating

Table 3. Selected Bond lengths (Å) and Angles (°) for 1[a]

Ru−N(1)	2.062(15)	Ru−N(1)#1	2.062(15)
Ru−N(2)	2.051(14)	Ru−N(2)#1	2.051(14)
Ru−N(3)	2.052(17)	Ru−N(3)#1	2.052(17)
O(1)−C(12)	1.21(3)	O(2)−C(13)	1.24(3)
N(1)−C(5)	1.34(2)	N(4)−C(11)	1.46(3)
N(1)−C(1)	1.34(3)	N(5)−C(12)	1.35(3)
N(2)−C(10)	1.34(2)	N(5)−C(14)	1.46(3)
N(2)−C(6)	1.35(2)	N(6)−C(13)	1.33(3)
N(3)−C(15)	1.31(3)	N(6)−C(11)	1.45(3)
N(3)−C(19)	1.36(3)	N(7)−C(13)	1.35(3)
N(4)−C(12)	1.33(3)	N(7)−C(14)	1.40(3)
N(2)#1−Ru−N(2)	173.0(8)	N(2)−Ru−N(1)	78.7(6)
N(2)#1−Ru−N(3)#1	88.4(6)	N(3)#1−Ru−N(1)	172.5(7)
N(2)−Ru−N(3)#1	97.0(6)	N(3)−Ru−N(1)	94.7(8)
N(2)#1−Ru−N(3)	97.0(6)	N(1)#1−Ru−N(1)	91.9(9)
N(2)−Ru−N(3)	88.4(6)	C(5)−N(1)−Ru	115.2(12)
N(3)#1−Ru−N(3)	78.9(12)	C(1)−N(1)−Ru	125.8(14)
N(2)#1−Ru−N(1)#1	78.7(6)	C(10)−N(2)−Ru	126.8(13)
N(2)−Ru−N(1)#1	96.4(6)	C(6)−N(2)−Ru	114.7(11)
N(3)#1−Ru−N(1)#1	94.7(8)	C(15)−N(3)−Ru	128.7(19)
N(3)−Ru−N(1)#1	172.5(7)	C(19)−N(3)−Ru	113.3(17)
N(2)#1−Ru−N(1)	96.4(6)	N(6)−C(11)−N(4)	111.7(17)
N(4)−C(12)−N(5)	110(2)	N(6)−C(13)−N(7)	109(2)
N(7)−C(14)−N(5)	113.5(18)	O(1)−C(12)−N(4)	125(3)
O(1)−C(12)−N(5)	125(2)	O(2)−C(13)−N(6)	125(3)
O(2)−C(13)−N(7)	125(2)		

[a] Symmetry transformations used to generate equivalent atoms: #1 $-x + 1/2, -y + 3/2, z$.

bipyridine nitrogen with the water molecule which further bonds to N−H group of the second molecule to generate zigzag chains when viewed down *a*-axis (Figure 2B). PLATON[19] calculations show that the solvent accessible void is 44 Å^3 per unit cell volume. The voids occupy about 1.6% of the crystal volume.

These variegated H-bonding interactions will be propagated to form secondary building units as the ruthenium ion chelates the bipyridine unit which will also depend on the number of BPG units to give rise to metallosupramolecular structural motifs which is evidenced in the crystal structure of **1** and **2**.

Crystal Structure of 1. A single crystal of **1** suitable for X-ray diffraction was grown by slow evaporation of compound in methanol–water solution at room temperature and crystallizes with lattice–water molecules in the tetragonal system with space group *P*42/*n*. The structure of the cationic building block of the composition $[Ru(phen)(BPG)_2]^{2+}$ **1** is depicted in Figure 3. Here the Ru(II) atom is coordinated to two BPG ligands and one phenanthroline ligand by the nitrogen atoms. The bulky urea groups prevent a close approach and the development of π-stacking interactions of adjacent phenanthroline groups. Selected crystallographic data parameters, bond lengths and angles are given in Tables 1 and 3, respectively. The coordination geometry of the RuN_6 chromophore is distorted from a regular octahedral with Ru−N ranging from 2.051 to 2.061 Å and Ru−N−Ru from 78 to 97° similar to that found in other analogous mixed ligand polypyridyl ruthenium complexes.[20]

Each cationic unit of **1** affords eight hydrogen bond donors (N-H) and four hydrogen bond acceptors (C=O) from the two BPG ligands which are involved in a variety of hydrogen bonds (Figure S2−S4 in the Supporting Information). The cationic units are arranged in a zigzag manner such that the phenanthroline units of the adjacent cationic units are exactly opposite and perpendicular to each other and the two BPG ligands hydrogen bond with the BPG ligands of the adjacent cationic molecules maximizing the number of hydrogen bonds with each other and also with the water molecules in order to stabilize the structure (Figure 4). The MOF formed packs efficiently via C−H···Cl, C−H···O, N−H···Cl, and N−H···O (Table S2 in the Supporting Information) interactions. The cations are surrounded by chlorine anions and water molecules showing a network of H-bonding (Figure 5 and Figure S5 in the Supporting Information) generating 3D MOF by a self-assembly process. PLATON[19] calculations show that the solvent accessible void is 210 Å^3 per unit cell volume. The voids occupy about 3.8% of the crystal volume.

A closer view of the association of water molecules with each other, chlorine anions and the MOF (N7, N4, O1, O2) forming water cluster is depicted in Figure 6.

Important bond distances and angles related to the water cluster are given in Table 4. In the water cluster some of the water molecules form H-bonds with the chlorine anions (Figure 4) with an average Cl···O distance of 2.75 Å, which further links to the MOF via H-bonding with N7, N4, O1, O2 atoms of the cationic unit. A wide variation in the hydrogen bonded O···O distances (2.61 to 2.99 Å), O···O···O angles (122 to 155°) (Table 4) attribute flexibility to the water molecules in this environment so that they can surround the cationic moiety. The thermal stability of the water molecules in compound **1** has been studied by TGA in N_2 atmosphere, which shows the weight loss steps with onset of water loss at about 40 °C and complete loss of water takes place up to 290 °C. Total weight loss in this temperature range is 15% (calculated weight loss

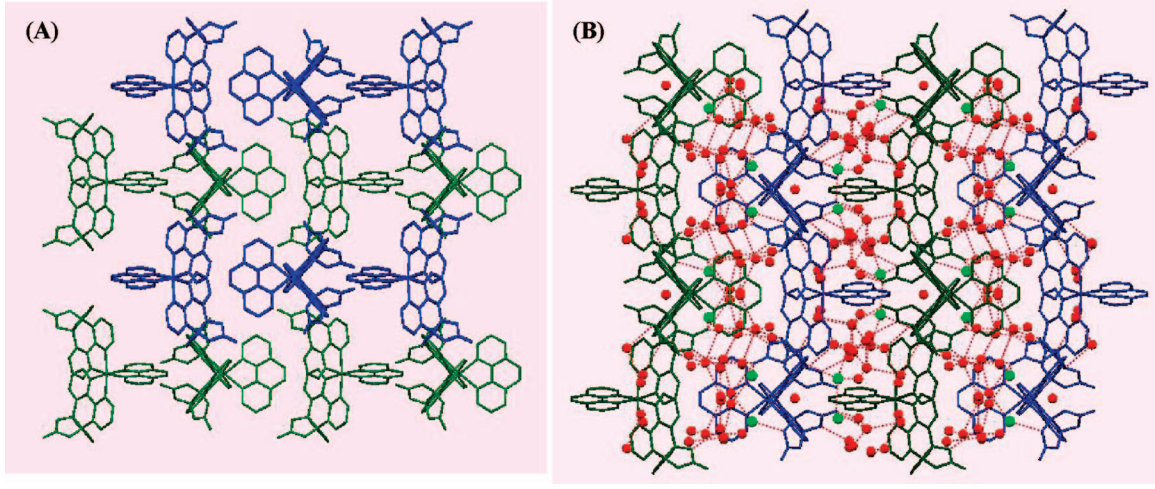

Figure 4. (A) Arrangement of the secondary building units when viewed down the *b*-axis (water and chlorine molecules are omitted for clarity); (B) the MOF structure of **1** viewed down the *b*-axis in the plane.

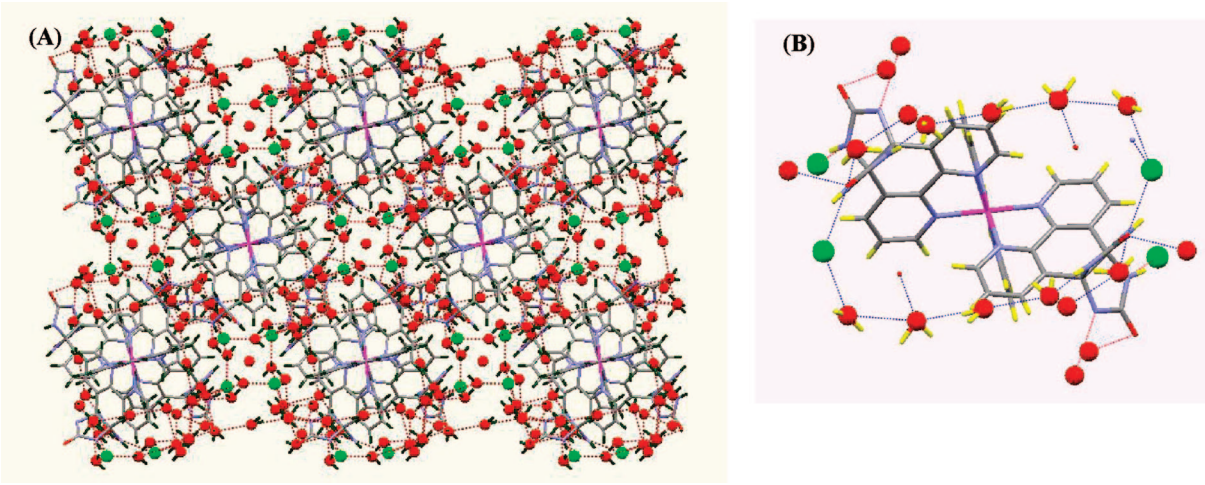

Figure 5. (A) The MOF structure of **1** viewed down the *c*-axis in the plane; (B) monomeric supramolecular synthon **1** surrounded by the water and chlorine molecules.

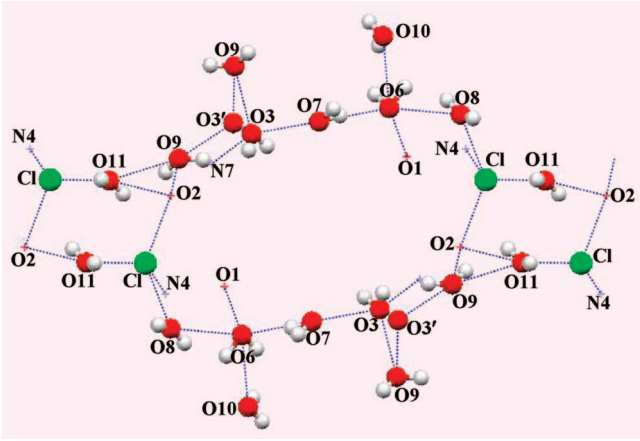

Figure 6. A network of the water molecules in **1** showing the association with MOF (N7, N4, O1, O2) and chlorine anions viewed down the *c*-axis.

Table 4. Geometrical Parameters of Hydrogen Bonds (Å, deg) for the Water Cluster in 1

Cl···O2	2.731	O6···O8	2.919
Cl···O8	2.753	O6···O7	2.955
Cl···O11	2.766	O6···O1	2.862
Cl···N4	2.921	O6···O10	2.941
O3···N7	2.947	O9···O5	2.772
O3···O7	2.595	O9···O2	2.808
O3···O9	2.643	O11···O9	2.828
O3′···O9	2.663	O11···O2	3.005
O3···O9···O11	141.96	O8···O6···O7	131.81
O3···O3′···O9	122.07	O7···O3···O3′	135.89
O6···O7···O3	155.05		

14.97%) corresponding to the loss of 8.8 water molecules. The framework begins to decompose above 290 °C (Figure S6 in the Supporting Information). Here in case of **1** the monomeric supramolecular synthon with two tectons is surrounded by the water molecules and chlorine anions which are rare in the vast area of research on the design and synthesis of a diverse metal organic framework structures. Recently, Custelcean et al. have demonstrated the selective inclusion of $Cl(H_2O)_4^-$ cluster in a MOF functionalized with carboxylic acid.[9j]

Crystal Structure of 2. Red colored rectangular single crystal of **2** suitable for X-ray diffraction was grown by slow evaporation of compound in dimethylsulfoxide solution at room

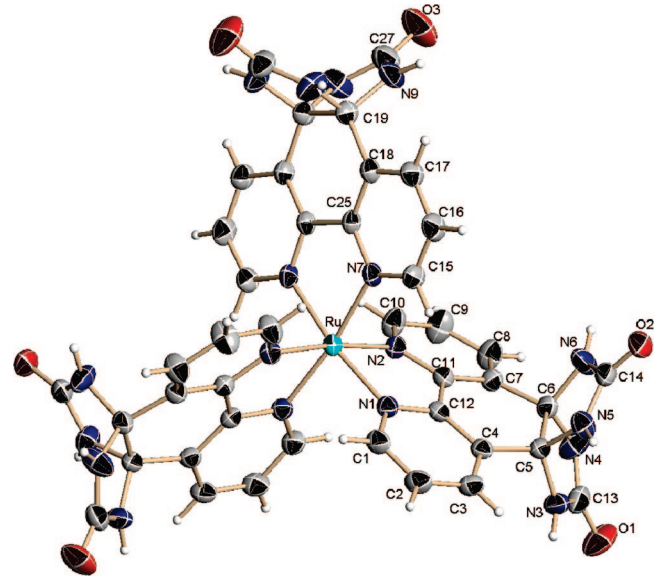

Figure 7. ORTEP diagram of the cationic building block **2** showing the atom numbering scheme (thermal ellipsoids are drawn at 50% probability).

temperature. The compound crystallizes in the monoclinic system with space group *C2/c*. Figure 7 shows the molecular structure of cationic building block of the composition $[Ru(BPG)_3]^{2+}$ **2**. The monomeric supramolecular synthon **2** having a 2-fold symmetry is composed of Ru(II) atom coordinated to three BPG ligands by the nitrogen atoms. The complex exhibits distorted octahedral geometry around the metal atom with Ru−N distances in the range 2.056(4)−2.072(4) Å, (Table 5) similar to that found in other analogous homoleptic polypyridyl ruthenium complexes.[20]

Each cationic building block of **2** has 12 H-bond donors and 6 H-bond acceptors which are involved in N−H···O, C−H···O, N−H···Cl, and C−H···Cl interactions (Figure S7 in the Supporting Information) to generate a self-assembled MOF forming channels into which mixed water−dimethylsulfoxide clusters are encapsulated (Figure 6A). Two of the BPG ligands are equivalent by symmetry denoted as X and X′ and third nonequivalent ligand BPG is referred to as Y. The central ruthenium atom and the ligand Y of the cationic building block are located on the C_2 axis. The ligand X shows hydrogen

Table 5. Bond Lengths [Å] and Angles [°] for 2[a]

Ru−N(1)	2.056(4)	O(1)−C(13)	1.236(6)
Ru−N(1)#1	2.056(4)	O(2)−C(14)	1.227(6)
Ru−N(2)	2.066(4)	O(3)−C(27)	1.216(7)
Ru−N(2)#1	2.066(4)	N(4)−C(6)	1.435(6)
Ru−N(7)	2.072(4)	N(5)−C(14)	1.358(7)
N(1)−C(1)	1.336(6)	N(5)−C(5)	1.462(6)
N(1)−C(12)	1.362(6)	N(6)−C(6)	1.453(6)
N(2)−C(10)	1.343(6)	N(7)−C(25)	1.351(6)
N(2)−C(11)	1.356(6)	N(7)−C(15)	1.353(6)
N(3)−C(13)	1.345(7)	N(9)−C(27)	1.368(8)
N(3)−C(5)	1.437(6)	N(10)−C(27)#1	1.351(7)
N(4)−C(13)	1.345(7)	N(10)−C(19)	1.444(6)
N(1)#1−Ru−N(1)	89.5(2)	N(2)#1−Ru−N(7)	94.12(14)
N(1)#1−Ru−N(2)#1	78.96(14)	N(2)−Ru−N(7)	90.99(14)
N(1)−Ru−N(2)#1	96.31(14)	N(1)#1−Ru−N(7)#1	96.47(14)
N(1)#1−Ru−N(2)	96.31(14)	N(1)−Ru−N(7)#1	171.33(14)
N(1)−Ru−N(2)	78.96(14)	N(2)#1−Ru−N(7)#1	90.99(14)
N(2)#1−Ru−N(2)	173.4(2)	N(2)−Ru−N(7)#1	94.12(14)
N(1)#1−Ru−N(7)	171.33 (14)	N(7)−Ru−N(7)#1	78.3(2)
N(1)−Ru−N(7)	96.47(14)		

[a] Symmetry transformations used to generate equivalent atoms: #1 $-x + 1, y, -z + 1/2$; #2 $-x + 1, -y + 1, -z + 1$.

bonding interactions with the other X′ and Y ligands of the adjacent cationic unit and vice-versa (Figure 8A,C). However the ligand Y shows hydrogen-bonding interactions with the ligand X′ of the adjacent cationic unit. Packing of the molecules when viewed down *b*-axis show zigzag arrangement, with channels in which solvent molecules and anions are sandwiched (Figure 8B). Cationic building blocks are connected through N−H···O interactions ranging from 2.84 to 2.94 Å forming a supramolecular 3D MOF (Table S3 in the Supporting Information). The cationic metal ensemble thus formed arrange themselves in layers so that the adjacent layers run in opposite directions forming channels separated by dimethylsulfoxide solvent molecules (Figure 8B). The chlorine anions lie along the walls of the cavity, while water molecules lie in the center of the cavity when viewed down *a*-axis. The inverted molecules come closer to form a cavity having disordered dimethylsulfoxide molecule at the center surrounded by chlorine anions and water molecules (Figure 8C).

A closer view of the mixed $(H_2O)_8(C_2H_6SO)_{2.5}$ cluster formed is depicted in Figure 9A, and the repeating unit of water cluster is shown in Figure 9B. An extensive array of intermolecular hydrogen bonds between the water molecules along with chloride anions and one and half molecules of the dimethylsulfoxide stabilizes the extended structure. Apart from the interactions with the solvent molecules and chlorine anions, mixed cluster is further hydrogen bonded to the cationic building blocks via N−H···O and O−H···O interactions (N4, N5, N6, O1, O3). This spatial arrangement of hydrophobic groups on one side and hydrophilic on the other, not only maintains the structural integrity of the hydrogen-bonding network within the water cluster but also aids in maximizing the cooperative hydrogen bonding with dimethylsulfoxide molecules.

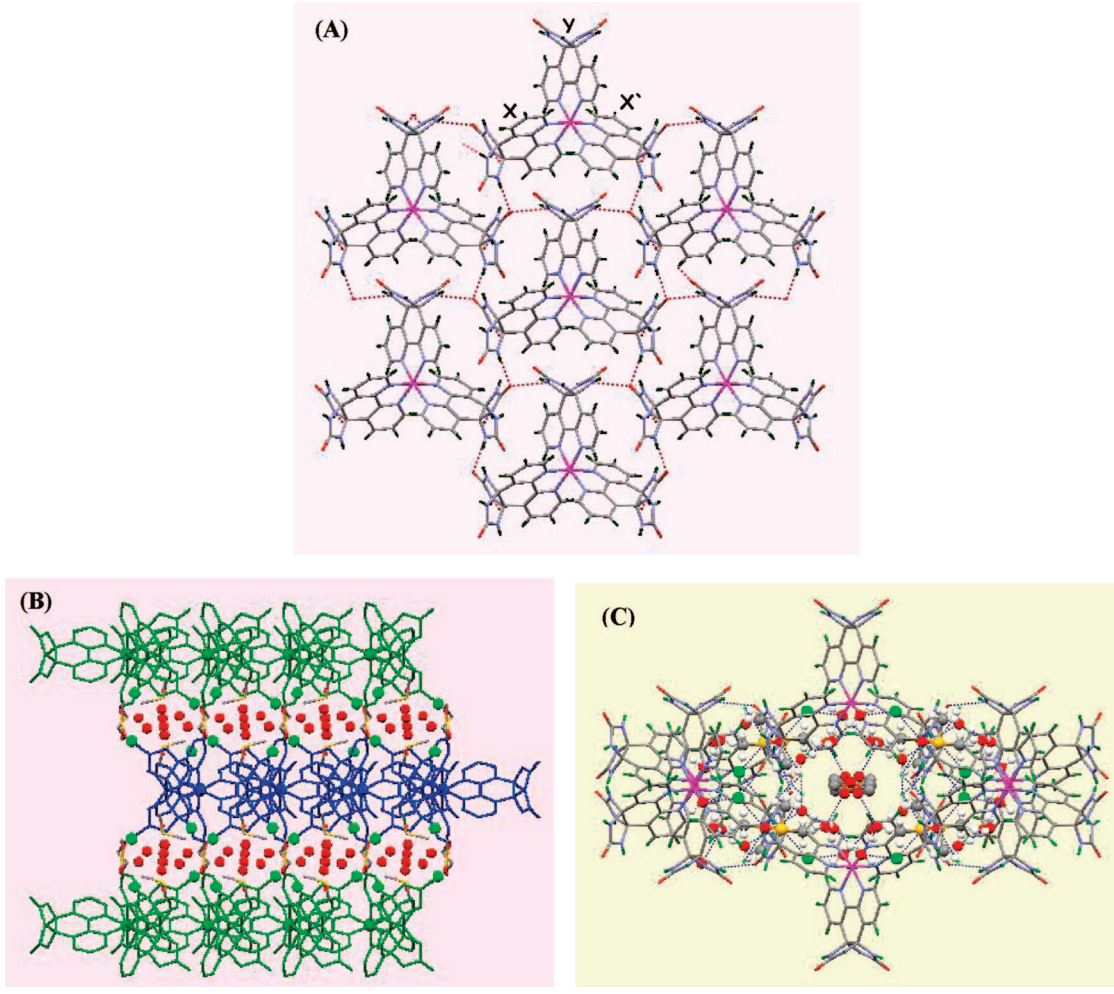

Figure 8. (A) The arrangement of cationic building units showing hydrogen-bonded network structure **2** viewed down the *c*-axis in the plane; (B) the MOF structure of **2** viewed down the *a*-axis in the plane; (C) the MOF structure of **2** viewed down the *c*-axis in the plane.

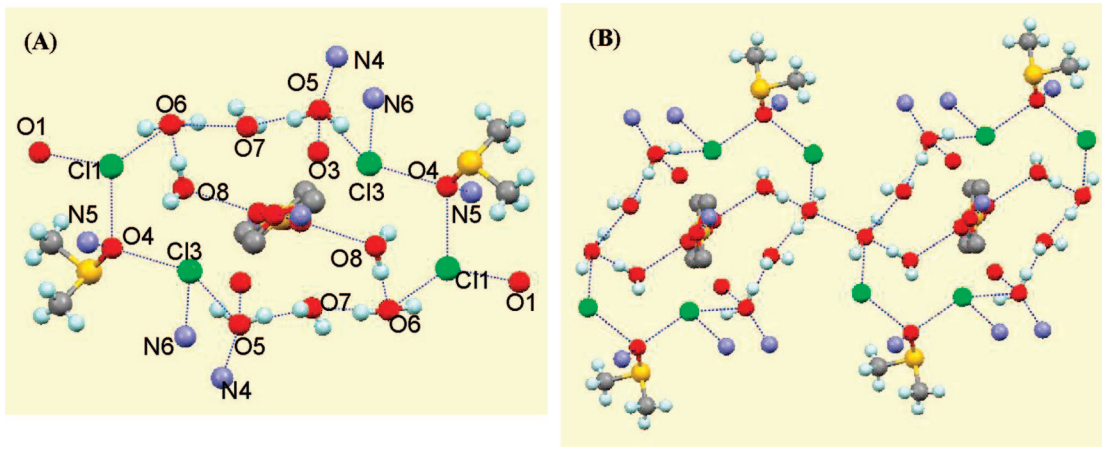

Figure 9. (A) A perspective view of mixed $(H_2O)_8(C_2H_6SO)_{2.5}$ cluster showing the association of water and dimethylsulfoxide molecules in compound **2** supported by the MOF (N4, N5, N6, O1, O3) and chlorine anions (Cl1, Cl3) via hydrogen bonds; (B) A view showing the network of water−dimethylsulfoxide cluster with the repeating unit bound to each other, MOF and chlorine atoms.

Table 6. Geometrical Parameters of Hydrogen Bonds (Å, °) for the Mixed Water−Dimethylsulfoxide−Water Cluster in 2

O5···O7	2.739	N6···Cl3	2.769
O6···O8	2.881	O1···Cl1	2.731
O6···O7	2.730	Cl1···O6	2.754
O2···N9	2.938	Cl1···O4	2.866
N3···O2	2.941	Cl3···O4	2.874
N5···O4	2.867	Cl3···O5	3.220
N4···O5	2.838		
O8···O6···O7	88.10	O3···O5···O7	99.51
O6···O7···O5	164.64	O10′···O8···O6	106.14

Important bond lengths and angles related to the mixed water−dimethylsulfoxide cluster are listed in Table 6. Each unit of mixed water−dimethylsulfoxide cluster is buttressed by chloride anions (Figure 9) on the two sides with the average Cl···O distances 2.89 Å, which also links the MOF via N−H···O distances. There is flexibility to the water molecules in this environment, so that they can be accommodated in the channels and at the same time can maximize the interactions among themselves. As far as we are aware this is one of the first example of mixed water−dimethylsulfoixde cluster encapsulated in a MOF, and such well-characterized mixed water-solvent clusters are very rare in the vast water cluster chemistry. Recently, Katti et al. characterized supramolecular water–methanol clusters in a novel phosphorus functionalized trimeric amino acid host.[18b] Winpenny et al. reported the water−acetonitrile−water cluster in which the two water molecules are coordinated to the metal center.[18c]

The thermal stability of the water molecules in compound **2** has been studied by TGA in air atmosphere which shows the continuous loss of water and dimethylsulfoxide at about 40 °C and complete loss at 300 °C after which it decomposes. Total weight loss in this temperature range is 14.16% (calculated weight loss 14.40%) corresponding to the loss of four water and one and half-dimethylsulfoxide molecules (Figure S10 in the Supporting Information).

In a previous study,[11a] we have observed a supramolecular self-assembled MOF architecture of $[Ru(bpy)_2(BPG)]Cl_2$ in which the two cations in the asymmetric unit arrange such that the BPG ligand from two cations face each other forming wide variety of hydrogen bonding networks resulting in channels running through the structure that encapsulates a tetradecameric water cluster, which, after dehydration, can be reabsorbed.

Thus, the formation of these structures depends on the stoichiometry of the ancillary bipyridine-glycoluril ligand which is further enhanced by the external conditions, such as solvent, resulting in a variety of diverse frameworks.

Conclusions

BPG ligand with inherent chelating ability and peripheral hydrogen bonding groups has been synthesized and structurally characterized, which on complexation with an inert metal such as ruthenium(II) gives rise to secondary building units. These secondary building units form diverse supramolecular motifs by variegated H-bonds depending upon the number of tectons and solvent molecules forming channels encapsulating unusual water clusters. The interactions of these mixed ruthenium(II) polypyridyl complexes with DNA are presently being investigated in our laboratory.

Acknowledgment. M.S.D. acknowledges Bhabha Atomic Research Centre (BARC) for providing a research fellowship through collaborative research scheme of Pune University - BARC, Mumbai, India. A.S.K. thanks University of Pune for partial funding.

Supporting Information Available: Crystallographic data for the structures BPG, **1**, and **2** have been deposited with the Cambridge Crystallographic Data Centre as Supplementary Publications CCDC reference number 662371 (BPG), 662370 (**1**) and 603105 (**2**). Copies of the data can be obtained free of charge on application to CCDC, 12 Union Road, Cambridge CB21EZ, U.K. (Fax: +(44) 1223-336-033; e-mail: deposit@ccdc.cam.ac.uk). Organic framework structure of BPG tecton (Figure S1), H-bonding parameters in BPG, **1** and **2** (Table S1−S3), cationic building block of the composition **1** $[Ru(phen)(BPG)_2]^{2+}$ showing N−H···O, N−H···Cl, C−H···O, and C−H···Cl interactions (Figure S2), molecular structure of compound **1** depicting cationic molecules showing N−H···O, N−H···Cl, C−H···O and C−H···Cl interactions with the core view of the water cluster and the chlorine anion (Figure S3, S4), the space filling model of the water and chloride anions surrounding the cationic building blocks forming channels when viewed down *c*-axis. (Figure S5), Thermogravimetric curve of compound **1** (Figure S6), cationic building block **2** of the composition $[Ru(BPG)_3]^{2+}$ (Figure S7), thermogravimetric curve of the Compound **2** (Figure S8). This information is available free of charge via the Internet at http://pubs.acs.org.

References

(1) (a) Desiraju, G. R. *Chem. Commun.* **2005**, 2995. (b) Saha, B. K.; Nangia, A. M.; Jaskolski, M. *CrystEngComm* **2005**, *7*, 355. (c) Burrows, A. D. *Struct. Bonding* **2004**, *108*, 55. (d) Beatty, A. M.

CrystEngComm **2001**, *51*, 1. (e) Braga, D. *Chem. Commun.* **2003**, 2751. (f) Biradha, K. *CrystEngComm* **2003**, *5*, 374. (g) Desiraju, G. R. *J. Mol. Struct.* **2003**, *656*, 5. (h) Desiraju, G. R. *Angew. Chem., Int. Ed. Engl.* **1995**, *34*, 2311. (i) Aakeröy, C. B.; Seddon, K. R. *Chem. Soc. Rev.* **1993**, *22*, 397. (j) Jeffery, G. A. In *An Introduction to Hydrogen Bonding*; Wiley: Chichester, 1997.

(2) (a) Robin, A. Y.; Fromm, K. M. *Coord. Chem. Rev.* **2006**, *250*, 2127. (b) Janiak, C. *Dalton Trans.* **2003**, 2781. (c) James, S. L. *Chem. Soc. Rev.* **2003**, *32*, 276. (d) Eddaoudi, M.; Moler, D. B.; Chen, B.; Reineke, T. M.; O'Keeffe, M.; Yaghi, O. M. *Acc. Chem. Res.* **2001**, *34*, 319.

(3) (a) Aakeroy, C. B.; Beatty, A. M. *Aust. J. Chem.* **2001**, *54*, 409. (b) Braga, D.; Grepioni, F. *Acc. Chem. Res.* **2000**, *33*, 601. (c) Tadokoro, M.; Nakasuji, K. *Coord. Chem. Rev.* **2000**, *198*, 205.

(4) Eddaoudi, M.; Kim, J.; Rosi, N.; Vodak, D.; Wachter, J.; O'Keeffee, M.; Yaghi, O. M. *Science* **2002**, *295*, 469.

(5) Boskovic, C.; Brechin, E. K.; Streib, W. E.; Folting, K.; Bollinger, J. C.; Hendrickson, D. N.; Christou, G. *J. Am. Chem. Soc.* **2002**, *124*, 3725.

(6) Bourne, S. A.; Lu, J.; Mondal, A.; Moulton, B.; Zaworotko, M. J. *Angew. Chem. Int. Ed.* **2001**, *40*, 2111.

(7) Davis, M. E. *Nature* **2002**, *417*, 813.

(8) Chui, S. S.-Y.; Lo, S. M. -F.; Charmant, J. P. H.; Orpen, A. G.; Williams, I. D. *Science* **1999**, *283*, 1148.

(9) (a) Jung, O.-S.; Kim, Y. J.; Lee, Y.-A.; Park, J. K.; Chae, H. K. *J. Am. Chem. Soc.* **2000**, *122*, 9921. (b) Muthu, S.; Yip, J. H. K.; Vittal, J. J. *J. Chem. Soc. Dalton. Trans.* **2002**, 4561. (c) Neogi, S.; Bharadwaj, P. K. *Cryst. Growth Des.* **2006**, *6*, 433. (d) Zhang, X.-M.; Fang, R.-Q.; Wu, H.-S. *Cryst. Growth Des.* **2005**, *5*, 1335. (e) Ghosh, S. K.; Bharadwaj, P. K. *Inorg. Chem.* **2004**, *43*, 6887. (f) Tao, J.; Ma, Z.-J.; Huang, R.-B.; Zheng, L.-S. *Inorg. Chem.* **2004**, *43*, 6133. (g) Liu, Q.-Y.; Xu, L. *CrystEngComm* **2005**, *7*, 87. (h) Neogi, S.; Savitha, G.; Bharadwaj, P. K. *Inorg. Chem.* **2004**, *43*, 3771. (i) Ghosh, S. K.; Ribas, J.; Bharadwaj, P. K. *CrystEngComm* **2004**, *6*, 250. (j) Custelcean, R.; Gorbunova, M. G. *J. Am. Chem. Soc.* **2005**, *127*, 16362. (k) Zheng, J.-M.; Batten, S. R.; Du, M. *Inorg. Chem.* **2005**, *44*, 3371. (l) Marivel, S.; Shimpi, M. R.; Pedireddi, V. R. *Cryst. Growth Des.* **2007**, *7*, 1791. (m) Kumar, D. K.; Jose, D. A.; Das, A.; Dastidar, P. *Inorg. Chem.* **2005**, *44*, 6933. (n) Kumar, D. K.; Das, A.; Dastidar, P. *Cryst. Growth Des.* **2007**, *7*, 205. (o) Kumar, D. K.; Jose, D. A.; Das, A.; Dastidar, P. *Chem. Commun.* **2005**, 4059. (p) Custelcean, R.; Moyer, B. A.; Bryantsev, V. S.; Hay, B. P. *Cryst. Growth Des.* **2006**, *6*, 555. (q) Hu, X.-X.; Xu, J.-Q.; Cheng, P.; Chen, X.-Y.; Cui, X.-B.; Song, J.-F.; Yang, G.-D.; Wang, T.-G. *Inorg. Chem.* **2004**, *43*, 2261, and references therein. (r) Zhang, X.-L.; Chen, X.-M. *Cryst. Growth Des.* **2005**, *5*, 617.

(10) (a) Tynan, E.; Jensen, P.; Lees, A. C.; Moubaraki, B.; Murray, K. S.; Kruger, P. E. *CrystEngComm* **2005**, *7*, 90. (b) Kato, M.; Kishi, S.; Wakamatsu, Y.; Sugi, Y.; Osamura, Y.; Koshiyama, T.; Hasegawa, M. *Chem. Lett.* **2005**, *34*, 1368. (c) Matthew, C. J.; Elsegood, M. R. J.; Bernardinelli, G.; Clegg, W.; Williams, A. F. *Dalton Trans.* **2004**, 492. (d) Goddard, R.; Hemalatha, B.; Rajasekharan, M. V. *Acta Crystallogr. C* **1990**, *46*, 33. (e) Tynan, E.; Jensen, P.; Kruger, P. E.; Lees, A. C.; Nieuwenhuyzen, M. *Dalton Trans.* **2003**, 1223. (f) Tynan, E.; Jensen, P.; Kelly, N. R.; Kruger, P. E.; Lees, A. C.; Moubaraki, B.; Murray, K. S. *Dalton Trans.* **2004**, 3440. (g) Tynan, E.; Jensen, P.; Kruger, P. E.; Lees, A. C. *Chem. Commun.* **2004**, 776. (h) Yajima, T.; Takamido, R.; Shimazaki, Y.; Odani, A.; Nakabayashi, Y.; Yamauchi, O. *Dalton Trans.* **2007**, 299. (i) Janiak, C.; Deblon, S.; Wu, H.-P.; Kolm, M. J.; Klufers, P.; Piotrowski, H.; Mayer, P. *Eur. J. Inorg. Chem.* **1999**, 1507. (j) Stephenson, M. D.; Hardie, M. J. *CrystEngComm* **2007**, 496. (k) Zhang, X.-M.; Wu, H.-S.; Chen, X.-M. *Eur. J. Inorg. Chem.* **2003**, 2959. (l) Wu, J.-Y.; Yeh, T.-T.; Wen, Y.-S.; Twu, J.; Lu, K.-L. *Cryst. Growth Des.* **2006**, *6*, 467. (m) Cargill Thompson, A. M. W.; Jeffrey, J. C.; Liard, D. J.; Ward, M. D. *J. Chem. Soc., Dalton Trans.* **1996**, 879.

(11) (a) Deshpande, M. S.; Kumbhar, A. S.; Puranik, V. G.; Selvaraj, K. *Cryst. Growth Des.* **2006**, *6*, 743. (b) Deshpande, M. S.; Kumbhar, A. A.; Kumbhar, A. S. *Inorg. Chem.* **2007**, *46*, 5450.

(12) Kurth, D. G.; Fromm, K. M.; Lehn, J. M. *Eur. J. Inorg. Chem.* **2001**, 1523.

(13) Yamada, M.; Tanaka, Y.; Yoshimoto, Y.; Kuroda, S. *Bull. Chem. Soc. Jpn.* **1992**, *65*, 1006.

(14) Elemans, J. A. A. W.; Gelder, R. D.; Rowan, A. E.; Nolte, R. J. M. *Chem. Commun.* **1998**, 1553.

(15) Krause, R. A. *Inorg. Chim. Acta* **1977**, *22*, 209.

(16) Sheldrick, G. M. *SHELX-97 Program for Crystal Structure Refinement*; University of Göttingen: Göttingen, Germany, 1997.

(17) Allen, G. H.; White, R. P.; Rillema, D. P.; Meyer, T. J. *J. Am. Chem. Soc.* **1984**, *106*, 2613.

(18) (a) Treadway, J. A.; Loeb, B.; Lopez, R.; Anderson, P. A.; Keene, F. R.; Meyer, T. J. *Inorg. Chem.* **1996**, *35*, 2242. (b) Raghuraman, K.; Katti, K. K.; Barbour, L. J.; Pillarsetty, N.; Barnes, C. L.; Katti, K. V. *J. Am. Chem. Soc.* **2003**, *125*, 6955. (c) Archibald, S. J.; Blake, A. J.; Parsons, S.; Schroder, M.; Winpenny, R. P. E. *J. Chem. Soc. Dalton Trans.* **1997**, 173.

(19) Spek, A. L. *PLATON-97*; University of Utrecht: Utrecht, The Netherlands, 1997.

(20) (a) Rillema, D. P.; Jones, D. S.; Levy, H. A. *J. Chem. Soc. Chem. Commun.* **1979**, 849. (b) Rillema, D. P.; Jones, D. S.; Woods, C.; Levy, H. A. *Inorg. Chem.* **1992**, *31*, 2935. (c) Rusanova, J. A.; Decurtins, S.; Rusanov, E. B.; Stoeckli - Evans, H. *Z. Kristallogr. NCS* **2002**, *217*, 571. (d) Bueu, J.; Stoll, A. *J. Acta. Crystallogr.* **1996**, *C52*, 1174. (e) Zou, X.- H.; Li, H.; Yang, G.; Deng, H.; Liu, J.; Li, R.- H.; Zhang, Q. - L.; Xiong, Y.; Ji, L.-N. *Inorg. Chem.* **2001**, *40*, 7091.

CG8000015